

Cover Page



Universiteit Leiden



The handle <http://hdl.handle.net/1887/36380> holds various files of this Leiden University dissertation

Author: Kooijman, Sander

Title: Neural control of lipid metabolism and inflammation : implications for atherosclerosis

Issue Date: 2015-11-18

2

INHIBITION OF THE CENTRAL MELANOCORTIN SYSTEM DECREASES BROWN ADIPOSE TISSUE ACTIVITY

Sander Kooijman

Mariëtte R. Boon

Edwin T. Parlevliet

Janine J. Geerling

Vera van de Pol

Johannes A. Romijn

Louis M. Havekes

Illiana Meurs

Patrick C.N. Rensen

Abstract

2

The melanocortin system is an important regulator of energy balance and MC4R deficiency is the most common monogenic cause of obesity. We investigated whether the relationship between melanocortin system activity and energy expenditure is mediated by brown adipose tissue (BAT) activity. Therefore, female APOE*3-Leiden.CETP transgenic mice were fed a Western-type diet for 4 weeks and infused intracerebroventricularly with the MC3/4R antagonist SHU9119 or vehicle for 2 weeks. SHU9119 increased food intake (+30%), body fat (+50%) and decreased energy expenditure by reduction in fat oxidation (-42%). In addition, SHU9119 impaired the uptake of VLDL-TG by BAT. In line with this, SHU9119 decreased uncoupling protein-1 levels in BAT (-60%) and induced large intracellular lipid droplets, indicative of severely disturbed BAT activity. Finally, SHU9119-treated mice pair-fed to the vehicle-treated group still exhibited these effects, indicating that MC4R inhibition impairs BAT activity independent of food intake. These effects were not specific to the APOE*3-Leiden.CETP background as SHU9119 also inhibited BAT activity in wild-type mice. We conclude that inhibition of central MC3/4R signaling impairs BAT function, which is accompanied by reduced energy expenditure thereby promoting adiposity. We anticipate that activation of MC4R is a promising strategy to combat obesity by increasing BAT activity.

Introduction

The hypothalamus is important in the regulation of energy balance. Activation of pro-opiomelanocortin neurons, *e.g.* by insulin or leptin, induces secretion of α -melanocyte-stimulating hormone, which in turn stimulates melanocortin -3 and -4 receptors (MC3R/MC4R) within the paraventricular nucleus to cause a negative energy balance (1). Accordingly, activation of central MC4R in rodent models results in anorexia and weight loss (2), whereas blockade or targeted gene disruption induces hyperphagia and obesity, even on regular chow diet (3,4). Loss-of-function mutations in MC4R are the most common monogenic form of obesity in humans and are associated with severe obesity in childhood (5). In addition, recent meta-analyses of genome-wide association studies identified common variants near MC4R to influence fat mass, obesity and obesity risk (6,7). These observations support an essential role for the melanocortin system in the regulation of energy homeostasis across mammalian species.

In addition to the effects of the melanocortin system on food intake, this system also affects energy balance via other pathways. This notion is supported by the observation that pharmacological inhibition of central MC4R by intracerebroventricular (*i.c.v.*) administration of the synthetic MC3/4R antagonist SHU9119 still increases body fat in pair-fed rats (8). Moreover, the peripheral effects of the central melanocortin system involves alterations in the activity of the sympathetic nervous system (SNS), as *i.c.v.* administration of the MC3/4R agonist MTII dose-dependently increases renal sympathetic activity in mice (9). Furthermore, ablation of neurons that produce agouti-related protein (AgRP), the endogenous antagonist for MC4R, in mice changes autonomic output into metabolic organs, accompanied by a changed respiratory exchange ratio (RER) indicating altered nutrient combustion (10). Additionally, chronic *i.c.v.* SHU9119 treatment in rats increases the RER (8), indicative of reduced lipid utilization. Interestingly, variants near and in the MC4R gene in humans are not only associated with an increased RER (8), but also with reduced total energy expenditure (EE) (11,12), underscoring the importance of the melanocortin system in the regulation of EE.

A recently discovered and highly important contributor to EE is brown adipose tissue (BAT). BAT contributes to EE by combusting high amounts of TG into heat, a process mediated by uncoupling protein-1 (UCP-1) (13). Interestingly, MC4R expressing neurons project onto BAT (14), indicating that BAT may mediate the association between MC4R signaling and EE. Therefore, the aim of this study was to evaluate the role of the melanocortin system in BAT activity. For this purpose, we inhibited melanocortin receptor signaling using the MC3/4R antagonist SHU9119 in APOE*3-Leiden.CETP transgenic mice, a well-established model for human-like lipoprotein metabolism.

Materials & Methods

2

Animals and diet

Female APOE*3-Leiden.CETP mice on a C57Bl/6J background (15) were bred at our institutional animal facility and housed under standard conditions with a 12-12 h light-dark cycle with *ad libitum* access to food and water unless stated otherwise. From 12-22 weeks after birth, mice were fed a Western-type diet containing 15% (w/w) cacao butter and 0.1% cholesterol (AB Diets, Woerden, The Netherlands) for the duration of the study, to increase plasma levels of apoB-containing lipoproteins thereby inducing a more human-like lipoprotein profile. After 4 weeks of run-in diet, mice were randomized into groups that received i.c.v. administration of artificial cerebrospinal fluid (vehicle) or SHU9119 (5 nmol/day; Bachem, Bubendorf, Germany) in vehicle during 14-17 days. Since SHU9119 induces hyperphagia (3), the effect of SHU9119 on BAT activity independent of food intake was also investigated by using an additional SHU9119-treated group that was pair-fed (SHU9119-pf) to the vehicle-treated group. To achieve pair-feeding, food intake of the *ad libitum* fed mice was monitored daily and pair-fed mice received surgery one day behind the control mice. The pair-feeding regimen consisted of giving the mice the average daily consumed food amount by the control mice, just before onset of darkness. To investigate the effect of SHU9119 independent of dyslipidemia induced by Western-type feeding of APOE*3-Leiden.CETP mice, a second experiment was performed using 15-week old male wild-type C57Bl/6J mice (Charles River, USA) that were housed under similar conditions, while being fed a regular chow diet. After 2 weeks of acclimatization, mice were randomized into three groups receiving, e.g. vehicle, SHU9119 and SHU9119-pf for 15 days. All animal experiments were approved by the institutional ethics committee on animal care and experimentation at Leiden University Medical Center.

Surgical procedure

For continuous i.c.v. administration of SHU9119 vs. vehicle, mice were sedated using a mixture of dexmedetomidine (0.5 mg/kg), midazolam (5 mg/kg) and fentanyl (0.05 mg/kg), and cannulas (Brain Infusion Kit 3, ALZET Cupertino, CA, USA) were stereotactically placed in the left lateral ventricle of the brain (coordinates: -0.45 mm anteroposterior, -1.00 mm lateral and 2.50 mm dorsoventral from bregma). Osmotic mini-pumps (Model 1004, Alzet, CA) attached to the cannula via a catheter were implanted subcutaneously on the back slightly posterior to the scapulae. The skin was sutured and the sedation was antagonized with a mixture of antiparnezol (2.5 mg/kg), flumanezil (0.5 mg/kg) and naloxon (1.2 mg/kg). Buprenorphine (0.9 µg) was used as pain killer. After the surgery, mice were housed individually and food intake and body weight were monitored on a daily basis. By filling the catheters with

vehicle, mice were allowed to recover for four days before actually receiving the assigned treatment for 17 days (collection of organs or VLDL production) or 14 days (indirect calorimetry and VLDL clearance).

Body composition

After 17 days of treatment, body composition (lean mass and fat mass) was determined in conscious mice using an EchoMRI-100 (EchoMRI, Houston, Texas).

Indirect calorimetry

During the first 5 days of treatment, oxygen uptake ($\dot{V} O_2$), carbon dioxide production ($\dot{V} CO_2$) and physical activity were measured in fully automatic metabolic cages (LabMaster System, TSE Systems, Bad Homburg, Germany). The average RER, EE, carbohydrate and fat oxidation rates were calculated as described previously (16).

Liver lipid staining and content

Liver samples were perfused with PBS, collected, snap frozen and stored at -80°C . Sections of $10\ \mu\text{m}$ were cut, fixed in 4% paraformaldehyde and stained with Oil-red-O and Mayer's hematoxylin. Lipids were extracted according to a modified protocol from Bligh and Dyer (17). In short, small liver pieces were homogenized in ice-cold methanol ($10\ \mu\text{L}/\text{mg}$ tissue). $1.8\ \text{mL}$ of $\text{CH}_3\text{OH}:\text{CHCl}_3$ (3:1, vol/vol) was added to $45\ \mu\text{L}$ of homogenate. After vigorous mixing and centrifugation, the supernatant was dried and suspended in 2% Triton X-100. Concentrations of hepatic TG, total cholesterol (TC) and phospholipids (PL) were measured using commercially available enzymatic kits for TG (11488872, Roche Diagnostics, Germany), TC (11489232, Roche Diagnostics, Mannheim, Germany) and PL (3009, Instruchemie, Delfzijl, the Netherlands). Liver lipids were expressed per milligram of protein, which was determined using the BCA protein assay kit (Thermo Scientific, Rockford, IL, USA).

VLDL production

After 17 days of treatment, after 4 h of fasting (from 8.00 h to 12.00 h), the VLDL production rate was assessed. Mice were sedated using a mixture of ventranquil (6.25 mg/kg), dormicum (6.25 mg/kg), and fentanyl (0.31 mg/kg). Subsequently, mice were injected intravenously (i.v.) with $100\ \mu\text{L}$ PBS containing $150\ \mu\text{Ci}$ Tran ^{35}S label to measure *de novo* apoB synthesis and blood samples were taken via tail bleeding ($t=0$). 30 min after injection of the Tran ^{35}S label, the mice received an i.v. injection of 500 mg of tyloxapol (Triton WR-1339, Sigma Aldrich, Germany) per kg body weight as 10% (w/w) solution in PBS, to block VLDL-TG clearance by lipoprotein lipase (LPL)-mediated TG hydrolysis. Additional blood samples were taken at $t=15$, 30, 60 and 90 min after tyloxapol injection and used for determination of plasma TG concentration. After 120 min, the mice were exsanguinated via the retro-orbital

plexus. VLDL was isolated from serum after density gradient ultracentrifugation and counted for incorporated ^{35}S -activity. VLDL particle size was determined using a Zetasizer (Malvern Instruments, Malvern, UK) and VLDL lipid composition was determined as described above.

VLDL clearance experiment

Glycerol tri[^3H]oleate ([^3H]TO) and [^{14}C]cholesteryl oleate ([^{14}C]CO) double-labeled VLDL-like emulsion particles (80 nm) were prepared as previously described (18). After 14 days of i.c.v. SHU9119 or vehicle treatment, mice were fasted for 4 h (from 8.00 h to 12.00 h) and injected i.v. with the radiolabeled emulsion particles (1.0 mg TG in 200 μL PBS) via the tail vein. At time points $t=2, 5, 10$ and 15 min after injection, blood was taken from the tail vein to determine the serum decay of both radiolabels. Immediately after the last blood withdrawal, mice were euthanized by cervical dislocation and perfused with ice-cold PBS for 5 min. Organs were harvested, weighed, and the uptake of ^3H and ^{14}C radioactivity was determined.

BAT histology

After 17 days of SHU9119 treatment, a part of interscapular BAT (iBAT) was fixed in 4% paraformaldehyde in PBS (pH 7.4) for 24 h, dehydrated and embedded in paraffin. 10 μm sections were cut, rehydrated and stained with Mayer's hematoxylin and eosin. To determine sympathetic activation of BAT a tyrosine hydroxylase (TH) staining was performed. To this end, sections were rehydrated and incubated 15 min with 10 mM citrate buffer (pH 6.0) at 120°C for antigen retrieval. Sections were cooled on ice, washed in PBS and PBS 0.1% Tween and incubated with 5% BSA/PBS for 60 min at room temperature. This was followed by overnight incubation with 1:2000 anti-TH (Abcam) primary antibody at 4°C. Next, sections were incubated with secondary antibody (anti-rabbit antibody, DAKO enVision TM) and stained with Nova Red. Nuclei were counterstained with Mayer's haematoxylin and sections were mounted on glass slides. Percentage of area positive for TH staining was quantified using Image J software.

BAT Western blot analysis

Another part of BAT was snap frozen and stored at -80°C. These BAT samples were homogenized in RIPA buffer, centrifuged and protein concentration was determined using the BCA protein assay kit (Thermo Scientific, Rockford, IL, USA). Samples were diluted and denatured for 5 min at 95°C after adding Laemmli Sample Buffer (1:1, vol/vol; Serva, Heidelberg, Germany). Proteins within homogenates (1 μg protein for UCP1 and 15 μg for p-CREB) were separated on a 10% SDS-page gel and subsequently transferred onto blotting membrane. The blotting membranes were then washed with PBS+0.1% Tween (PBS+T), blocked with 5% milk powder in PBS+T and incubated

O/N at 4°C with the first antibody (anti-UCP-1 rabbit polyclonal; Ab U6382, Sigma Aldrich or anti-p-CREB; Cell). After washing (PBS-T) the second antibody (anti-rabbit IgG HRP conjugate; 1:5,000; Promega, Madison, WI, USA) was added. After another wash with PBS-T and PBS, SuperSignal Western Blot Enhancer (Thermo Scientific, Rockford, IL, USA) was added to the blotting membranes after which they were analyzed with Bio-Rad Quantity One.

BAT gene expression analysis

A part of iBAT from wild-type C57Bl/6J mice treated with vehicle or SHU9119, was snap frozen and stored at -80°C for gene expression analysis and protein analysis (see above). Total RNA was isolated using TriPure (Roche) according to the manufacturer's instructions. 1 µg of total RNA was reverse-transcribed using M-MLV reverse transcriptase (Promega, Madison, WI, USA). Real-time PCR was carried out on a CFX96 PCR machine (Bio-Rad) using IQ SYBR-Green Supermix (Bio-Rad). Melt curve analysis was included to assure a single PCR product was formed. Expression levels were normalized using β 2-microglobulin as housekeeping gene.

Body temperature

In four wild-type C57Bl/6J mice per group, temperature transponders (IPTT-300, BMDS) were implanted subcutaneously in the clavicular region. Every three days body temperature was recorded using a compatible Smart Probe (BMDS).

Statistical analysis

Differences between groups were determined using independent sample T-tests for normally distributed data and Mann-Whitney U tests for non-normal distributed data. Serum decay in the VLDL clearance experiment was analyzed using repeated measurements ANOVA with a Tukey's Post-Hoc test. Probability values less than 0.05 were considered statistically significant. Data are presented as means \pm SEM.

Results

SHU9119 increases body weight and fat mass independent of food intake

APOE*3-Leiden.CETP mice were treated i.c.v. with SHU9119 or vehicle for 17 days. In *ad libitum* fed mice, throughout the treatment period, SHU9119 consistently increased food intake (on average 4.04 ± 0.21 vs. 3.18 ± 0.13 g/day, $p < 0.01$) (**Figure 1A**), concomitantly with an increased body weight gain (after 17 days: 6.68 ± 0.58 vs. 0.70 ± 0.14 g, $p < 0.001$). Obviously, SHU9119 also increased body weight in pair-fed mice when compared to vehicle-treated mice (4.14 ± 0.45 vs. 0.70 ± 0.14 g, $p < 0.01$) (**Figure 1B**) indicating that the SHU9119-induced weight gain is independent of food

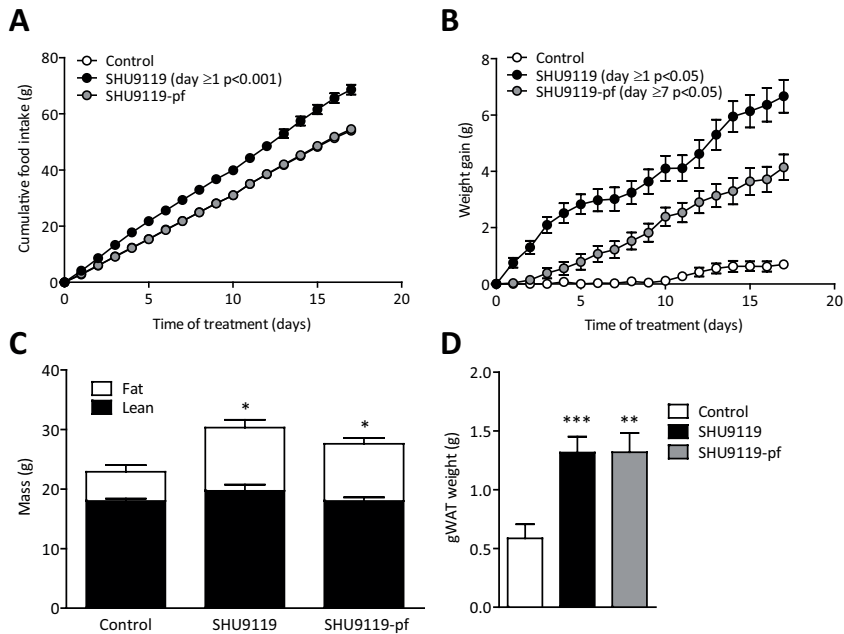


Figure 1 – SHU9119 increases body weight and fat mass independent of food intake. APOE*3-Leiden.CETP mice were treated intracerebroventricularly with vehicle (n=21) or SHU9119 (5 nmol/day) while being fed *ad libitum* (n=21) or being pair-fed (pf) to the vehicle-treated group (n=22). Food intake (**A**) and body weight gain (**B**) were monitored on a daily basis. After 17 days of treatment, lean and fat mass were measured in a random selection of the mice (n=3-4 per group) using EchoMRI (**C**). Part of the mice were used for the collection of organs, and weight of gonadal white adipose tissue was determined (n=10-11 per group) (**D**). Values are means \pm SEM. *p<0.05, **p<0.01, ***p<0.001 compared to control.

intake. Determination of body composition using EchoMRI revealed that SHU9119 increased body weight under both *ad libitum* feeding and pair-fed conditions due to a selective increase in fat mass (10.6 \pm 1.2 and 9.6 \pm 1.0 vs. 4.9 \pm 1.1 g, p<0.05) (**Figure 1C**). The SHU9119-induced increase in body weight and fat mass was accompanied by an increase in gonadal white adipose tissue (gWAT) weight, both in *ad libitum* feeding conditions (+124%; 1.32 \pm 0.13 vs. 0.59 \pm 0.12 g, p<0.001) and pair-fed conditions (+124%; 1.32 \pm 0.16 vs. 0.59 \pm 0.12 g, p<0.01) (**Figure 1D**). SHU9119 increased plasma TG levels in pair-fed mice, while it decreased total cholesterol levels in both *ad libitum* and pair-fed mice (**Supplemental Figure 1**).

In a first experiment, we did observe a large increase in plasma TG levels upon 17 days of SHU9119 treatment under *ad libitum* conditions (**Supplemental Figure 1A**), which would be consistent with reduced uptake of TG by BAT. However, in a subsequent

study the SHU9119-induced increase in plasma TG only reached significance under pair-fed conditions (**Supplemental Figure 1B**).

SHU9119 reduces whole body fat oxidation independent of food intake

Since SHU9119 induced fat accumulation independent of food intake, we reasoned that SHU9119 likely affected EE. Therefore, we next assessed the effect of SHU9119 on energy metabolism. Fully automated metabolic cages were used during the first 5 days of treatment in order to prevent a potential confounding effect of differences in body weight. Indeed, in *ad libitum* fed mice, SHU9119 decreased EE (-10%; 23.7 ± 0.3 vs. 26.4 ± 0.2 cal/h/g fat-free mass [FFM], $p < 0.05$) (**Figure 2A**) and increased RER (0.92 ± 0.01 vs. 0.88 ± 0.00 $p < 0.01$) (**Figure 2B**). These effects were not caused by an effect on carbohydrate oxidation (**Figure 2C**) but rather by a large reduction in fat oxidation (-43%; 5.1 ± 1.0 vs. 8.9 ± 0.3 cal/h/g FFM, $p < 0.001$) (**Figure 2D**). SHU9119 also reduced activity of the animals (-46%; 67 ± 6 vs. 123 ± 5 A.U., $p < 0.05$; **Figure 2E**). Strikingly, the effects of SHU9119 in pair-fed mice, as compared to the control group, were essentially similar as in *ad libitum* fed mice with respect to EE (23.9 ± 0.1 cal/h/g FFM; $p < 0.01$), RER (0.91 ± 0.01 ; $p < 0.01$), fatty acid oxidation (5.3 ± 0.5 cal/h/g FFM; $p < 0.001$) and activity (75 ± 3 A.U.; $p < 0.05$). Apparently, SHU9119 reduced EE, because of reduced fat oxidation and independent of food intake, as well as a lower locomotor activity.

SHU9119 induces hepatic steatosis due to increased food intake

Since the liver is an important player in TG storage and secretion, we evaluated the effect of SHU9119 on liver weight and TG content as well as on hepatic VLDL-TG secretion. SHU9119 induced hepatomegaly as evidenced by increased liver weight (+85%; 2.17 ± 0.11 vs. 1.17 ± 0.06 g, $p < 0.001$) (**Figure 3A**) and aggravated hepatic steatosis, as shown by a selective increase in liver TG (+57%; 689 ± 33 vs. 439 ± 37 nmol/mg protein, $p < 0.001$) (**Figure 3B**) and neutral lipid staining (**Figure 3C**). However, the effects of SHU9119 on the liver were fully attributed to the induction of hyperphagia, as hepatomegaly and hepatic steatosis were not induced under pair-fed conditions (**Figure 3A-D**). SHU9119 did not affect the VLDL-TG production rate in mice that were either fed *ad libitum* (3.39 ± 0.14 mmol/L/h) or pair-fed (3.61 ± 0.37 mmol/L/h) as compared to control mice (3.59 ± 0.29 mmol/L/h) (**Figure 3D,E**). The VLDL-apoB production rate was slightly decreased in SHU9119-treated mice, but not in pair-fed SHU9119-treated mice (**Figure 3F**). In line with these observations, SHU9119 did not affect VLDL particle size (**Figure 3G**), VLDL composition (**Figure 3H**), or hepatic expression of the genes *Apob*, *Mttp*, *Dgat2* involved in VLDL synthesis (not shown). Taken together, SHU9119 induced hepatic steatosis secondary to its induction of hyperphagia and without affecting VLDL-TG secretion.

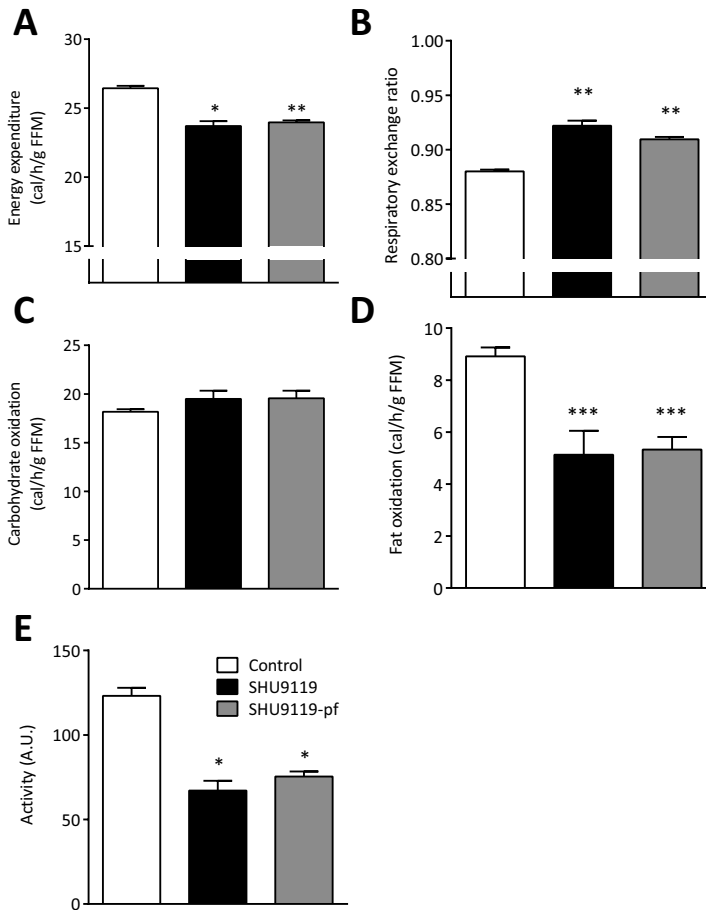


Figure 2 – SHU9119 lowers energy expenditure by reducing fat oxidation independent of food intake. APOE*3-Leiden.CETP mice were treated intracerebroventricularly with vehicle (n=9) or SHU9119 (5 nmol/day) while being fed *ad libitum* (n=6) or being pair-fed (pf) to the vehicle-treated group (n=9). During the first 5 days of treatment, mice were housed in fully automated metabolic cages. Energy expenditure (**A**), respiratory exchange ratio (**B**), carbohydrate oxidation (**C**) and fat oxidation (**D**) were calculated from O₂ uptake and CO₂ excretion. Values are means ± SEM. *p<0.05, **p<0.01, ***p<0.001 compared to control.

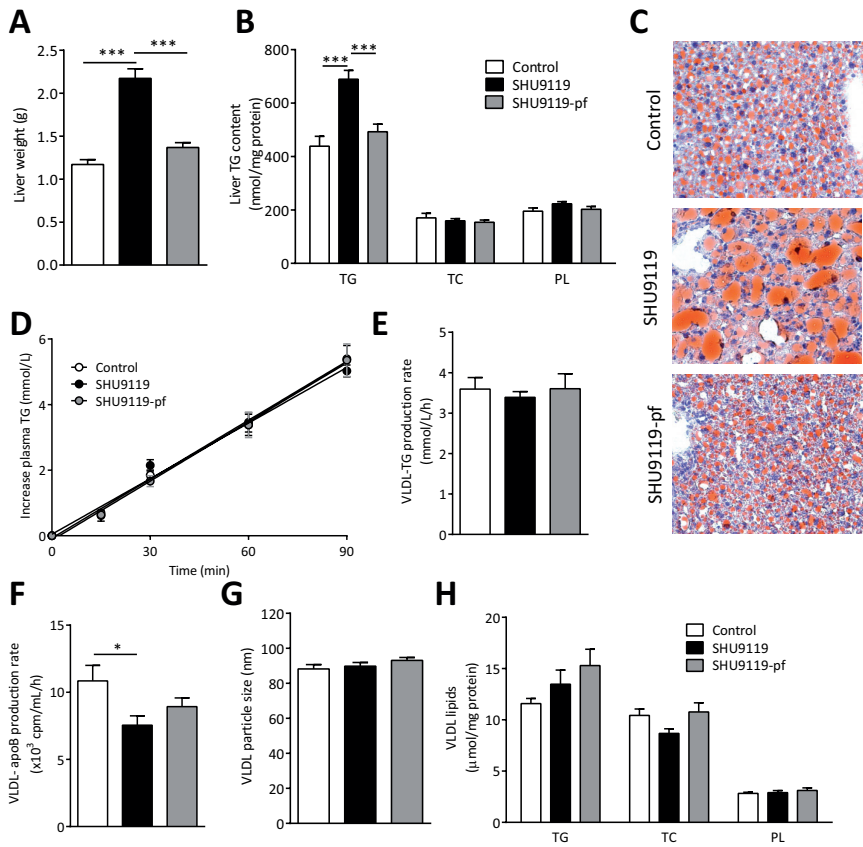


Figure 3 – SHU9119 induces hepatomegaly and steatosis only in *ad libitum* fed mice. APOE*3-Leiden.CETP mice were treated intracerebroventricularly with vehicle (n=21) or SHU9119 (5 nmol/day) while being fed *ad libitum* (n=21) or being pair-fed (pf) to the vehicle-treated group (n=20). After 17 days of treatment, part of the mice were sacrificed (n=10-11 per group) to collect organs and determine liver weight (A), and to determine liver content of triglycerides (TG), total cholesterol (TC) and phospholipids (PL) (B). Frozen liver samples were sectioned and stained with a neutral lipid staining (Oil-red-O) and hematoxylin, and representative pictures are shown (C). The remaining mice (n=8-10 per group) were 4 h fasted, consecutively injected with Trans³⁵S label and tyloxapol, and blood samples were drawn up to 90 min after tyloxapol injection. Plasma TG concentration was determined and plotted as the increase in plasma TG relative to t=0 (D). The rate of TG production was calculated from the slopes of the curves from the individual mice (E). After 120 min, the total VLDL fraction was isolated by ultracentrifugation and the rate of newly synthesized VLDL-ApoB was determined (F). The VLDL fractions were assayed for particle size (G) and lipid content (H). Values are means ± SEM. *p<0.05, ***p<0.001 compared to control.

SHU9119 induces brown adipose tissue dysfunction independent of food intake

Since BAT strongly contributes to fat oxidation and total energy expenditure, we subsequently determined the effect of SHU9119 treatment on BAT function. SHU9119 treatment increased BAT weight in *ad libitum* fed mice (+50%; 0.15 ± 0.01 vs. 0.10 ± 0.01 g, $p < 0.01$) and tended to increase BAT weight in pair-fed animals (+24%; 0.13 ± 0.01 g, $p = 0.06$) (**Figure 4A**). Strikingly, SHU9119 dramatically increased intracellular lipid droplet size in BAT in both *ad libitum* fed and pair-fed mice (**Figure 4B**), along with reduced sympathetic innervation of BAT as evidenced by reduced tyrosine hydroxylase (*i.e.* the rate-limiting enzyme in norepinephrine synthesis) (-53%; $p < 0.001$ and -43%; $p < 0.001$) (**Figure 4C-D**) and reduced phosphorylation of CREB (-22%; $p < 0.05$ and -15%; *n.s.*) (**Figure 4E**), a downstream target of $\beta 3$ -adrenergic signaling. Accordingly, largely reduced UCP-1 protein levels in BAT (-61%; $p < 0.001$ and -61%, $p < 0.001$) were observed (**Figure 4F**). These data imply that SHU9119 decreases BAT activity independent of food intake, likely due to lower sympathetic innervation of BAT, and this may result in decreased burning of intracellularly stored TG and, as a consequence, larger intracellular lipid droplet size.

To assess the capacity of BAT to take up VLDL-TG, we next determined the effect of SHU9119 on the kinetics of *i.v.* injected [^3H]TO and [^{14}C]CO double-labeled VLDL-like emulsion particles after 14 days of treatment. SHU9119 impaired the plasma decay of [^3H]TO (**Figure 4G**) and [^{14}C]CO (**Figure 4I**) under *ad libitum* fed conditions, and that of [^{14}C]CO under pair-fed conditions (**Figure 4I**). At 15 min after injection, the distribution of radiolabels over the organs was assessed. In control mice, the uptake of [^3H]TO-derived activity by BAT ($31.6 \pm 8.0\%$ /g) was much higher than the uptake by liver (~4-fold), muscle (~25-fold) and WAT (~25-fold), indicating that BAT is highly metabolically active compared to other organs. Interestingly, SHU9119 tended to selectively decrease the uptake of [^3H]TO by BAT in the *ad libitum* fed group, and significantly did so in mice pair-fed to the control group (-57%; $13.7 \pm 1.9\%$ of injected dose/g; $p < 0.05$) (**Figure 4H**), most likely as a consequence of reduced hydrolysis of VLDL-TG. Indeed, in the control group, as compared to the ^3H -label, the uptake of the ^{14}C -label was much lower in BAT (~10-fold), muscle (~4-fold), heart (~3-fold) and WAT (~3-fold), while the uptake of ^{14}C -label was higher in liver (~3-fold). This pattern is compatible with selective delipidation of the VLDL-like emulsion particles in plasma by the LPL-expressing tissues (*i.e.* uptake of ^3H activity), with subsequent uptake of the core remnant by the liver (*i.e.* uptake of ^{14}C activity). SHU9119 treatment tended to reduce the uptake of [^{14}C]CO in the liver of both *ad libitum* fed mice (-20%; $20.8 \pm 3.6\%$ /g; $p = 0.11$) and pair-fed mice (-11%; $23.1 \pm 1.5\%$ /g; $p = 0.25$) as compared to the control group ($26.1 \pm 2.1\%$ /g), whereas it decreased the uptake of [^{14}C]CO by BAT (*ad libitum* fed: -39%; $p = 0.24$; pair-fed: -57%; $p < 0.01$) (**Figure 4J**).

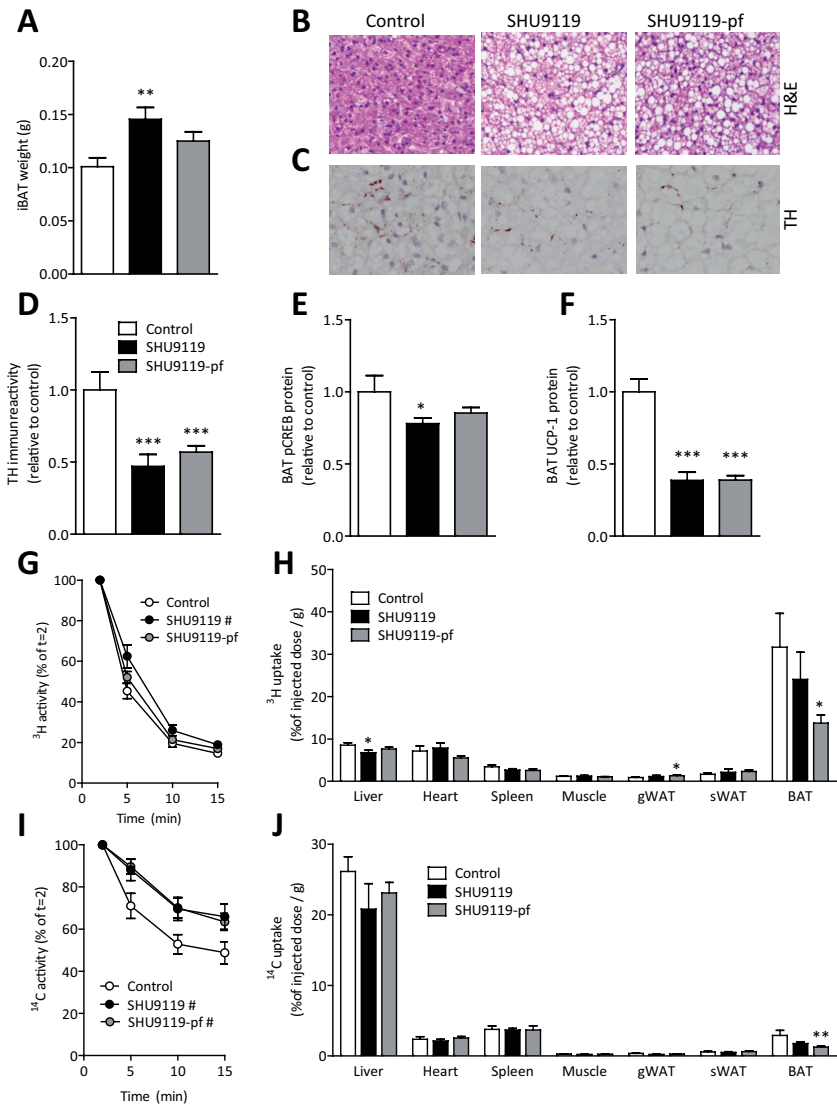


Figure 4 – SHU9119 causes malfunction of brown adipose tissue. APOE³-Leiden.CETP mice were treated intracerebroventricularly with vehicle (n=21) or SHU9119 (5 nmol/day) while being fed *ad libitum* (n=21) or being pair-fed (pf) to the vehicle-treated group (n=22). After 17 days of treatment, part of the mice were sacrificed (n=10-11 per group) and interscapular brown adipose tissue (iBAT) was quantitatively removed. iBAT was examined for weight (A), morphology, as assessed by hematoxylin and eosin (H&E) staining, (B) and tyrosine hydroxylase (TH) content (C,D). In iBAT, protein content of phosphorylated CREB (E) and UCP-1 (F) were determined. In a second experiment, after 14 days of i.c.v. treatment with vehicle (n=8) or SHU9119 (5 nmol/day) while being fed *ad libitum* (n=5) or being pf to the vehicle-treated group (n=9), mice were 4h fasted and consecutively injected with [³H]T0 and [¹⁴C]CO-labeled VLDL-like emulsion particles. Plasma [³H]T0 (G) and [¹⁴C]CO (H) were determined at the indicated time points and plotted relative to the dosage at t=2 min. At 15 min after injection, organs were isolated and uptake of the ³H-activity (I) and ¹⁴C-activity (J) was determined. Values are means ± SEM. #p<0.05, *p<0.05, **p<0.01, ***p<0.001 compared to control.

SHU9119 also induces brown adipose tissue dysfunction independent of dyslipidemia

To investigate the inhibitory effects of SHU9119 on BAT activity independent of dyslipidemia induced by Western-type diet feeding in APOE*3-Leiden.CETP mice, we next repeated experiments in wild-type mice that were fed a regular chow diet. Again, SHU9119 consistently increased food intake (on average 4.97 ± 0.29 vs. 4.10 ± 0.26 g/day, $p < 0.05$) (**Figure 5A**) accompanied by an increase in body weight gain (5.43 ± 0.58 vs. 0.21 ± 0.24 g, $p < 0.001$) (**Figure 5B**). As with the APOE*3-Leiden.CETP mice, administration of SHU9119 in wild-type mice increased body weight gain in pair-fed animals (1.29 ± 0.32 g, $p < 0.05$) (**Figure 5B**), due to a selective increase in fat mass (**Figure 5C**). Histological analysis revealed increased lipid accumulation in BAT upon SHU9119 treatment (**Figure 5D**), especially in the *ad libitum* fed mice in which 51±14% of the total area consisted of lipids ($p < 0.001$) (**Figure 5E**). In addition, SHU9119 tended to reduce tyrosine hydroxylase content in BAT in both *ad libitum* and pair-fed mice (-32% and -42%, respectively) (**Figure 5F**), accompanied by reduced phosphorylation of CREB (-32%, $p < 0.01$ and -52%, $p < 0.001$ respectively) (**Figure 5G**), supporting reduced sympathetic innervation of BAT. Again, SHU9119 markedly reduced UCP-1 protein content in BAT in both *ad libitum* and pair-fed mice (-54%, $p < 0.001$ and -64%, $p < 0.001$ respectively) (**Figure 5H**). SHU9119 resulted in lower body temperature in both *ad libitum* (35.9 ± 0.32 °C, $p < 0.01$), and pair-fed (35.6 ± 0.47 °C, $p < 0.05$) animals as compared to vehicle treated mice (36.7 ± 0.46 °C) (**Figure 5I-J**), which is in line with reduced BAT thermogenesis. We next assessed the capacity of BAT to take up VLDL-TG upon SHU9119 treatment. Again, SHU9119 lowered uptake of [³H]TO-derived activity from VLDL-like emulsion particles by BAT In *ad libitum* fed mice compared to vehicle treated animals (-80%; $p < 0.001$). Interestingly, in pair fed animals this effect was not observed (**Figure 5K**). Accordingly, gene expression of the lipolytic enzyme *Lpl* was decreased in *ad libitum* fed mice (-70%; $p < 0.001$), but not in pair fed mice (**Figure 5L**). These data suggest that lower local hydrolysis of TG-rich lipoprotein like particles may well underlie the lower uptake of TG by BAT upon SHU9119 treatment. Altogether, SHU9119 inhibits BAT activity in both hyperlipidemic APOE*3-Leiden.CETP mice and normolipidemic wild-type mice.

Discussion

The melanocortin system is an important regulator of energy balance and MC4R deficiency is the most common monogenic cause of obesity. BAT recently emerged as an important player in energy expenditure by combusting high amounts of TG towards heat. In addition, MC4R expressing neurons project onto BAT (14). Hence, the association between MC4R and energy expenditure may be mediated by BAT. In the current study we aimed to evaluate the direct effect of the melanocortin system

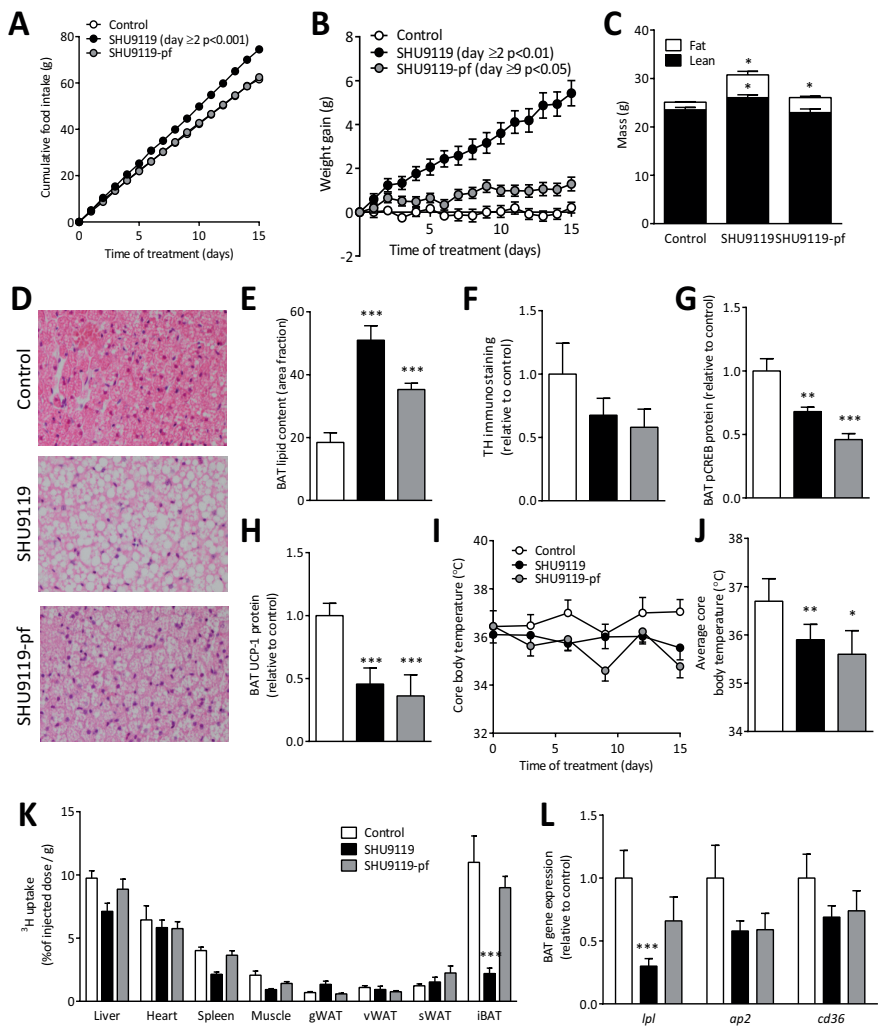


Figure 5 – SHU9119 induces brown adipose tissue dysfunction independent of dyslipidemia. Wild-type C57Bl/6J mice were treated intracerebroventricularly with vehicle (n=9) or SHU9119 (5 nmol/day) while being fed *ad libitum* (n=10) or being pair-fed (pf) to the vehicle-treated group (n=9). Food intake (A) and body weight (B) were monitored on a daily basis. After 15 days, body composition was determined using echo-MRI (C). Core body temperature was measured every 3 days using subcutaneously implanted temperature transponder (D) and average core body temperature was calculated (E). On histological level tyrosine hydroxylase (TH) immunoreactivity was determined (F) and BAT protein levels of phosphorylated CREB (G) and UCP-1 (H) were measured using Western blots. Before scarification, after 4h of fasting, mice were injected with ³H]TO-labeled VLDL-like emulsion particles and organs were isolated 15 min after injection. Uptake of the ³H-activity (I) was determined. On BAT, an H&E staining (J) was performed to quantify lipid content (K) and on frozen sections were used to determine gene expression (L). Values are means ± SEM. *p<0.05, **p<0.05, ***p<0.001 compared to control.

on BAT activity. For this purpose, we inhibited the central melanocortin system using the MC3/4R synthetic antagonist SHU9119 in APOE*3-Leiden.CETP mice. We found that i.c.v. administration of SHU9119 decreased EE and BAT activity, concomitant with selectively impaired uptake of TG from plasma by BAT, independent of food intake.

Both in *ad libitum* as well in pair-fed conditions, SHU9119 treatment increased body weight and WAT mass. These data are in line with those of Nogueiras *et al.* (8), who attributed weight gain and adiposity upon SHU9119 treatment to an increase in both lipid uptake as well as TG synthesis for storage in WAT. Accordingly, we found enhanced uptake of TG by gWAT after a bolus injection of double-labeled VLDL-like emulsion particles. Though the increase in TG uptake by gWAT may have seemed small when expressed per gram tissue, the total depot of gWAT may contribute to a marked absolute TG uptake by the tissue. We also showed that in *ad libitum* fed conditions, SHU9119 induced ectopic lipid deposition in the liver, manifested by hepatomegaly and hepatic steatosis. Hepatic steatosis did not develop in pair-fed mice, indicating that this effect is a direct consequence of SHU9119-induced hyperphagia. Similar effects on the liver are observed after 4 days of i.c.v. SHU9119 treatment in rats (19) and in MC4R deficient mice, which in addition develop steatohepatitis when fed a high-fat diet and have therefore been proposed as a novel mouse model for non-alcoholic steatohepatitis (NASH) (20). Although hepatic steatosis could promote the secretion of hepatic lipid as VLDL (21), SHU9119 did not increase the VLDL-TG production, VLDL-size or composition of newly synthesized VLDL. Our data corroborate those of Stafford *et al.*(22) who showed that a single i.c.v. injection of 15 µg SHU9119 does not affect VLDL-TG production in rats. Of note, ApoB production was decreased in *ad libitum* fed SHU9119 treated animals, which may be the consequence of the hepatic steatosis. These data corroborate previous observations that steatosis, by inducing ER stress, inhibits the hepatic production of apoB100 (23), which can result in production of large lipid-rich VLDL particles (24).

Because SHU9119 was able to increase body adiposity independent of a change in food intake, we reasoned that SHU9119 reduced EE. Indeed, by performing studies with metabolic cages we confirmed that inhibition of the central melanocortin system reduced EE. Besides decreasing locomotor activity, SHU9119 selectively reduced fat oxidation, whereas carbohydrate oxidation remained unaffected. This reduction in fat oxidation and total EE occurred independently of food intake and before changes in body weight were observed, indicative of a causal relation between reduced energy expenditure and the induction of obesity. Likewise, a previous study has shown that 7 days of i.c.v. injections with SHU9119 in rats increased the RER and thereby decreased fat utilization independent of food intake (8). As locomotor activity was not affected in that study, reduced fat oxidation may be dominant over the effect of decreased locomotor activity in the decrease in EE. In addition, MC4R-deficient humans also display an increase in RER (8). Taken together, we suggest that, in

general, inhibition of the melanocortin system results in a shift towards decreased metabolic use of lipids leading to elevated fat deposition in WAT.

Since BAT is a highly active metabolic tissue involved in EE and regulation of weight gain, we next proposed that the reduction in fat oxidation could be largely attributed to decreased activity of BAT. Indeed, in both *ad libitum* and pair-fed conditions in Western-type diet fed APOE*3-Leiden.CETP mice, analysis of BAT revealed that SHU9119 largely increased intracellular lipid stores and decreased the protein level of the UCP-1, both indicative of reduced BAT activity (25). These data corroborate previous findings showing that chronic i.c.v. treatment of *ad libitum* fed rats with SHU9119 lowered BAT temperature during the night (26). Moreover, 7 daily i.c.v. injections of AgRP, the endogenous antagonist for MC4R, decreased *Ucp1* gene expression in pair-fed rats (27), while acute i.c.v. injections of GLP-1, which indirectly stimulates MC4R, increased BAT thermogenesis by increasing activity of the sympathetic fibers towards BAT (28). Accordingly, since the activity of BAT is dependent on SNS outflow from the hypothalamus (29,30), reduced sympathetic output from the hypothalamus towards BAT is the likely mechanism by which inhibition of the central melanocortin system reduced BAT activity. We observed reduced sympathetic output towards BAT as evidenced by decreased levels of tyrosine hydroxylase, the rate limiting enzyme in norepinephrine synthesis, and decreased phosphorylation of CREB, a downstream target of β 3-adrenergic signaling, in BAT upon SHU9119 treatment. Thus, these data support a major role for BAT in the reduced EE and enhanced weight gain of central MC4R inhibition. However, based on these data, we cannot exclude the involvement of other metabolic tissues such as liver and WAT in the development of the disadvantageous metabolic phenotype.

Interestingly, in the Western type diet-fed APOE*3-Leiden.CETP mice we provided evidence that SHU9119 lowered both β -oxidation and VLDL-TG uptake by BAT, while lipid accumulation was markedly enhanced. This suggests that the lower β -oxidation upon SHU9119 treatment was more pronounced than the reduced VLDL-TG uptake by the tissue. It would make physiological sense if the reduction in VLDL-TG uptake by BAT occurred as a secondary mechanism to compensate for the diminished TG combustion by the tissue. Indeed, this is supported by the study performed in chow-fed wild-type C57Bl/6J mice. While both the *ad libitum* fed and pair-fed animals developed marked lipid accumulation in BAT upon SHU9119 treatment, only the *ad libitum* fed mice exhibited lower TG uptake by BAT. Of note, the lipid accumulation in BAT was less pronounced in the chow pair-fed C57Bl6/J mice as compared to the Western-type diet pair-fed APOE*3-Leiden.CETP mice, perhaps due to the lower fat content of the chow diet. It is, therefore, likely that especially brown adipocytes that become saturated with lipids lower their TG uptake as a secondary mechanism, for instance by downregulation of *Lpl* expression resulting in lower VLDL-TG hydrolysis.

Indeed, in the study with C57Bl6/J mice *Lpl* was downregulated only in the SHU9119 mice that were fed *ad libitum*.

Recently, Bartelt *et al.* (13) identified BAT as a major organ involved in plasma VLDL-TG clearance, with 24 hours of cold induction resulting in normalisation of plasma TG levels in hypertriglyceridemic mice. To investigate the effects of decreased BAT activity on plasma lipid levels, dyslipidemic APOE*3-Leiden.CETP mice were used in the first set of experiments. In a first experiment, we did observe a large increase in plasma TG levels upon 17 days of SHU9119 treatment under *ad libitum* conditions (**Supplemental Figure 1A**), which would be consistent with reduced uptake of TG by BAT. However, in a subsequent study the SHU9119-induced increase in plasma TG only reached significance under pair-fed conditions (**Supplemental Figure 1B**). Likewise, i.c.v. infusion of the MC4R synthetic antagonist HS104 also failed to increase plasma TG levels in pair-fed rats (31). It should be noted that MC4R deficient mice have only modestly increased plasma TG levels compared to control mice (+30%) (32), implying that partial inhibition of MC4R by SHU9119 may be insufficient to significantly increase plasma TG levels. In heterozygous MC4R-deficient subjects, plasma TG levels are increased (1.7 vs. 1.3 mmol/L) (33), indicating that the melanocortin system does play a role in the regulation of plasma VLDL-TG levels in humans.

Recently, Perez-Tilve *et al.* (34) demonstrated that inhibition of the central melanocortin neurons by either ghrelin or SHU9119 in wild-type mice increased circulating cholesterol, related to a decreased hepatic expression of SR-BI involved in the selective hepatic uptake of HDL-cholesteryl esters. In our study in APOE*3-Leiden.CETP mice with a human-like lipoprotein metabolism, SHU9119 did not rather decrease total cholesterol levels (**Supplemental Figure 1**) despite decreased hepatic SR-BI expression (**Supplemental Figure 2**). This is likely due to the expression of human CETP that provides an alternative route for the clearance of HDL-cholesterol, as CETP expression in SR-BI-deficient mice also precludes an increase in HDL-cholesterol (35). In addition, this could be related to an increased output of cholesterol in the feces as well as a somewhat reduced output of cholesterol from the liver within VLDL. Likewise, humans with heterozygous MC4R deficiency also do not have increased cholesterol levels (33), pointing to a species-dependent effect of MC4R function on HDL-cholesterol levels.

In conclusion, inhibition of central MC3/4R signaling by SHU9119 reduces BAT activity thereby reducing the uptake and combustion of VLDL-TG by BAT. As a consequence, excess lipids are stored in WAT (**Figure 6**). We anticipate that MC4R agonists that are currently in development to combat obesity, increase energy expenditure through activation of BAT.

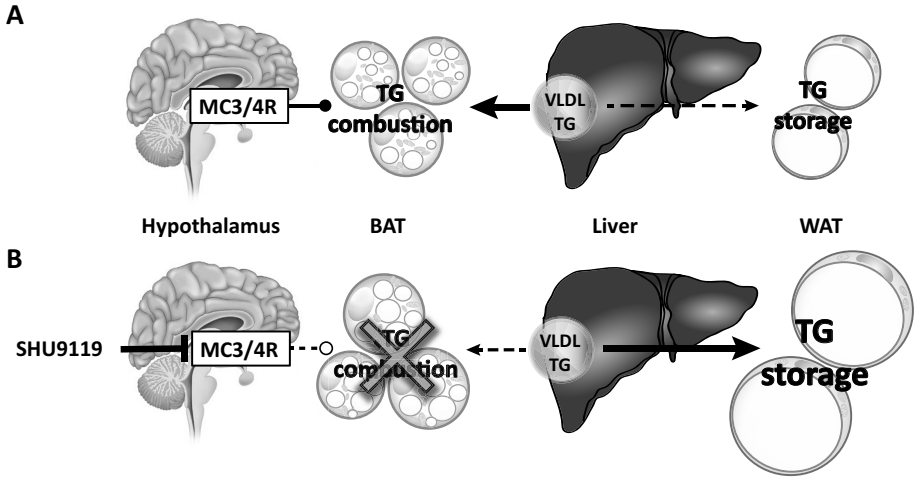


Figure 6 – Proposed model of the effect of SHU9119 on peripheral triglyceride metabolism. Under physiological conditions MC3/4R signalling is required for basal combustion of VLDL-derived triglycerides (TG) in brown adipose tissue (BAT), preventing storage of excess TG in WAT (A). Inhibition of central MC3/4R signaling by SHU9119 reduces BAT activity, thereby reducing the uptake and combustion of VLDL-TG by BAT. As a consequence, excess TG is stored in WAT, independent of SHU9119-induced hyperphagia (B).

Acknowledgements

We acknowledge the support from 'the Netherlands CardioVascular Research Initiative: the Dutch Heart Foundation, Dutch Federation of University Medical Centers, the Netherlands Organisation for Health Research and Development and the Royal Netherlands Academy of Sciences' for the GENIUS project 'Generating the best evidence-based pharmaceutical targets for atherosclerosis' (CVON2011-19). PCN Rensen is an Established Investigator of the Netherlands Heart Foundation (grant 2009T038).

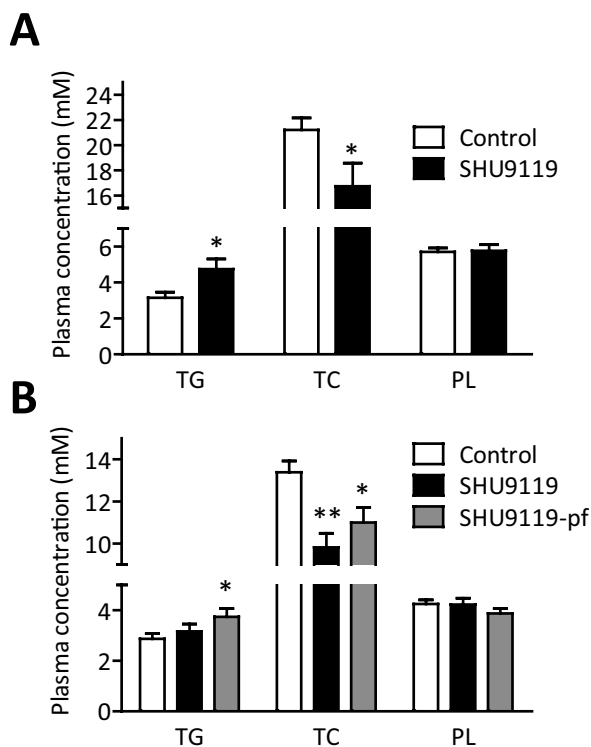
References

- Garfield, A. S., Lam, D. D., Marston, O. J. *et al.* (2009) Role of central melanocortin pathways in energy homeostasis. *Trends Endocrinol Metab* 20, 203-215.
- Nargund, R. P., Strack, A. M., & Fong, T. M. (2006) Melanocortin-4 receptor (MC4R) agonists for the treatment of obesity. *J Med Chem* 49, 4035-4043.
- Fan, W., Boston, B. A., Kesterson, R. A. *et al.* (1997) Role of melanocortinergic neurons in feeding and the agouti obesity syndrome. *Nature* 385, 165-168.
- Huszar, D., Lynch, C. A., Fairchild-Huntress, V. *et al.* (1997) Targeted disruption of the melanocortin-4 receptor results in obesity in mice. *Cell* 88, 131-141.
- Farooqi, I. S., Keogh, J. M., Yeo, G. S. *et al.* (2003) Clinical spectrum of obesity and mutations in the melanocortin 4 receptor gene. *N Engl J Med* 348, 1085-1095.
- Loos, R. J., Lindgren, C. M., Li, S. *et al.* (2008) Common variants near MC4R are associated with fat mass, weight and risk of obesity. *Nat Genet* 40, 768-775.
- Xi, B., Chandak, G. R., Shen, Y. *et al.* (2012) Association between common polymorphism near the MC4R gene and obesity risk: a systematic review and meta-analysis. *PLoS One* 7, e45731.
- Nogueiras, R., Wiedmer, P., Perez-Tilve, D. *et al.* (2007) The central melanocortin system directly controls peripheral lipid metabolism. *J Clin Invest* 117, 3475-3488.
- Rahmouni, K., Haynes, W. G., Morgan, D. A. *et al.* (2003) Role of melanocortin-4 receptors in mediating renal sympathoactivation to leptin and insulin. *J Neurosci* 23, 5998-6004.
- Joly-Amado, A., Denis, R. G., Castel, J. *et al.* (2012) Hypothalamic AgRP-neurons control peripheral substrate utilization and nutrient partitioning. *EMBO J* 31, 4276-4288.
- Cole, S. A., Butte, N. F., Voruganti, V. S. *et al.* (2010) Evidence that multiple genetic variants of MC4R play a functional role in the regulation of energy expenditure and appetite in Hispanic children. *Am J Clin Nutr* 91, 191-199.
- Krakoff, J., Ma, L., Kobes, S. *et al.* (2008) Lower metabolic rate in individuals heterozygous for either a frameshift or a functional missense MC4R variant. *Diabetes* 57, 3267-3272.
- Bartelt, A., Bruns, O. T., Reimer, R. *et al.* (2011) Brown adipose tissue activity controls triglyceride clearance. *Nat Med* 17, 200-205.
- Voss-Andreae, A., Murphy, J. G., Ellacott, K. L. *et al.* (2007) Role of the central melanocortin circuitry in adaptive thermogenesis of brown adipose tissue. *Endocrinology* 148, 1550-1560.
- Westerterp, M., van der Hoogt, C. C., de, H. W. *et al.* (2006) Cholesteryl ester transfer protein decreases high-density lipoprotein and severely aggravates atherosclerosis in APOE*3-Leiden mice. *Arterioscler Thromb Vasc Biol* 26, 2552-2559.
- Van Klinken, J. B., van den Berg, S. A., Havekes, L. M. *et al.* (2012) Estimation of activity related energy expenditure and resting metabolic rate in freely moving mice from indirect calorimetry data. *PLoS One* 7, e36162.
- BLIGH, E. G. & DYER, W. J. (1959) A rapid method of total lipid extraction and purification. *Can J Biochem Physiol* 37, 911-917.
- Rensen, P. C., Herijgers, N., Netscher, M. H. *et al.* (1997) Particle size determines the specificity of apolipoprotein E-containing triglyceride-rich emulsions for the LDL receptor versus hepatic remnant receptor in vivo. *J Lipid Res* 38, 1070-1084.
- Wiedmer, P., Chaudhary, N., Rath, M. *et al.* (2012) The HPA axis modulates the CNS melanocortin control of liver triacylglyceride metabolism. *Physiol Behav* 105, 791-799.
- Itoh, M., Suganami, T., Nakagawa, N. *et al.* (2011) Melanocortin 4 receptor-deficient mice as a novel mouse model of nonalcoholic steatohepatitis. *Am J Pathol* 179, 2454-2463.
- Adiels, M., Taskinen, M. R., Packard, C. *et al.* (2006) Overproduction of large VLDL particles is driven by increased liver fat content in man. *Diabetologia* 49, 755-765.

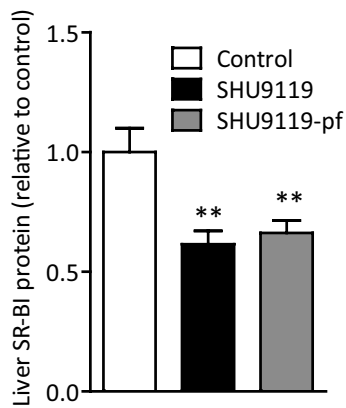
22. Stafford, J. M., Yu, F., Printz, R. *et al.* (2008) Central nervous system neuropeptide Y signaling modulates VLDL triglyceride secretion. *Diabetes* 57, 1482-1490.
23. Ota, T., Gayet, C., & Ginsberg, H. N. (2008) Inhibition of apolipoprotein B100 secretion by lipid-induced hepatic endoplasmic reticulum stress in rodents. *J Clin Invest* 118, 316-332.
24. Werner, A., Havinga, R., Bos, T. *et al.* (2005) Essential fatty acid deficiency in mice is associated with hepatic steatosis and secretion of large VLDL particles. *Am J Physiol Gastrointest Liver Physiol* 288, G1150-G1158.
25. Carobbio, S., Rosen, B., & Vidal-Puig, A. (2013) Adipogenesis: new insights into brown adipose tissue differentiation. *J Mol Endocrinol*
26. Verty, A. N., Allen, A. M., & Oldfield, B. J. (2010) The endogenous actions of hypothalamic peptides on brown adipose tissue thermogenesis in the rat. *Endocrinology* 151, 4236-4246.
27. Small, C. J., Kim, M. S., Stanley, S. A. *et al.* (2001) Effects of chronic central nervous system administration of agouti-related protein in pair-fed animals. *Diabetes* 50, 248-254.
28. Lockie, S. H., Heppner, K. M., Chaudhary, N. *et al.* (2012) Direct control of brown adipose tissue thermogenesis by central nervous system glucagon-like peptide-1 receptor signaling. *Diabetes* 61, 2753-2762.
29. Bartness, T. J., Vaughan, C. H., & Song, C. K. (2010) Sympathetic and sensory innervation of brown adipose tissue. *Int J Obes (Lond)* 34 Suppl 1, S36-S42.
30. Morrison, S. F., Madden, C. J., & Tupone, D. (2012) Central control of brown adipose tissue thermogenesis. *Front Endocrinol (Lausanne)* 3.
31. Baran, K., Preston, E., Wilks, D. *et al.* (2002) Chronic central melanocortin-4 receptor antagonism and central neuropeptide-Y infusion in rats produce increased adiposity by divergent pathways. *Diabetes* 51, 152-158.
32. Iqbal, J., Li, X., Chang, B. H. *et al.* (2010) An intrinsic gut leptin-melanocortin pathway modulates intestinal microsomal triglyceride transfer protein and lipid absorption. *J Lipid Res* 51, 1929-1942.
33. Greenfield, J. R., Miller, J. W., Keogh, J. M. *et al.* (2009) Modulation of blood pressure by central melanocortinergic pathways. *N Engl J Med* 360, 44-52.
34. Perez-Tilve, D., Hofmann, S. M., Basford, J. *et al.* (2010) Melanocortin signaling in the CNS directly regulates circulating cholesterol. *Nat Neurosci* 13, 877-882.
35. Hildebrand, R. B., Lammers, B., Meurs, I. *et al.* (2010) Restoration of high-density lipoprotein levels by cholesteryl ester transfer protein expression in scavenger receptor class B type I (SR-BI) knockout mice does not normalize pathologies associated with SR-BI deficiency. *Arterioscler Thromb Vasc Biol* 30, 1439-1445.

Supplementary appendix

2



Supplemental Figure 1 – Effect of SHU9119 on plasma lipid levels. **(A)** In a first experiment, APOE*3-Leiden.CETP mice were treated intracerebroventricularly with vehicle (n=10) or SHU9119 [5 nmol/day] (n=7). After 17 days of treatment, blood was drawn after a 4 h fast (from 8.00 h to 12.00 h) via tail vein bleeding in paraoxon-coated capillary tubes to prevent *ex vivo* lipolysis and assayed for triglycerides (TG), total cholesterol (TC) and phospholipids (PL) using commercially available enzymatic kits for TG (11488872, Roche Diagnostics, Germany), TC (11489232, Roche Diagnostics, Mannheim, Germany) and PL (3009, Instruchemie, Delfzijl, the Netherlands). **(B)** In a second experiment, mice were treated i.c.v. with vehicle (n=21) or SHU9119 (5 nmol/day) while being fed *ad libitum* (n=21) or being pair-fed (pf) to the vehicle-treated group (n=22). Plasma lipids were determined after 4 h of fasting. Values are means \pm SEM. *p<0.05, **p<0.01 compared to control.



Supplemental Figure 2 – Effect of SHU9119 on hepatic SR-BI protein levels. APOE*3-Leiden. CETP mice were treated intracerebroventricularly with vehicle (n=21) or SHU9119 (5 nmol/day) while being fed *ad libitum* (n=21) or being pair-fed (pf) to the vehicle-treated group (n=20). After 17 days of treatment, part of the mouse groups were sacrificed (n=10-11 per group) to collect organs and determine hepatic SR-BI protein levels. Values are means \pm SEM. **p<0.01 compared to control.

